PHYSICAL REVIEW D **76,** 031502(R) (2007)

Microscopic 8-quark study of the antikaon-nucleon-nucleon systems

P. Bicudo

CFTP, Dep. Física, Instituto Superior Técnico, Av. Rovisco Pais, 1049-001 Lisboa, Portugal

(Received 3 January 2007; revised manuscript received 25 June 2007; published 30 August 2007)

We study the possibility of binding eight quarks in a molecular hadronic system composed of two nucleons and an antikaon, with the quantum numbers of a hexaquark flavor, in particular, with strangeness -1, isospin $1/2$, parity -, baryonic number 2, and two possible spins, 0 or 1. We discuss the possible production of this hadron in the experiments which are presently investigating hot topics like the Θ^+ pentaquark or the K^- deeply bound in nuclei. The $K^- \bullet N$ interactions and the coupling to other channels are computed microscopically from a confining and chiral invariant quark model resulting in local plus separable Gaussian potentials. The $N \bullet N$ interactions used here are the state of the art Nijmegen potentials. The binding energy and the decay rate of the $K^- \bullet N$ and $K^- \bullet N \bullet N$ systems are computed with configuration space variational methods.

DOI: 10.1103/PhysRevD.76.031502 PACS numbers: 14.65.−q, 12.39.Fe, 14.20.Pt, 14.40.Aq

I. INTRODUCTION

Here we study the binding energy of a possible molecular antikaon, nucleon, and nucleon three-body system. Importantly, from a hadronic perspective, a bound $K^- \bullet N \bullet N$ can be at most reduced to a hexaquark, an exotic system. In a nuclear perspective, the deep binding of antikaons in nuclei has been predicted and is also actively searched. A bound $K^- \bullet N \bullet N$ would constitute a simple antikaon-nucleus system, the ${}^{2}_{K^-}H$.

Moreover, the $K^- \bullet N \bullet N$ can be formed with antikaon (K^-) deuteron ($p \bullet n$) scattering. Other exotic tetraquarks, pentaquarks, or hexaquarks are also very plausible, but they are all harder to produce experimentally because they would need at least strangeness and charm. The several experiments dedicated to pentaquark searches (where not only the kaon, but also the antikaon may interact with nuclei), or to antikaon-nuclear binding at RCNP, JLab, KEK, DAFNE, and at many other laboratories, are already able to search for the proposed $K^- \bullet N \bullet N$. In particular evidence for $K^- \bullet N \bullet N$ has already been found by the FINUDA collaboration at DAFNE [1,2]. In Fig. 1 different possible production mechanisms are depicted. They are similar to the $\Lambda(1405)$ production mechanisms, except that the K^- scatters on a deuterium nucleus, not on a hydrogen nucleus. The process in Fig. 1(a) is only possible if the width of the $K^- \bullet N \bullet N$ is of the order of its binding energy. The process in Fig. 1(b) is always possible, but it is suppressed by the electromagnetic coupling. Processes in Figs. 1(c) and 1(d) are dominant. The production process (c) should occur in experiments designed for the production of the pentaquark Θ^+, where the K^- has sufficient energy to create a π. The production process (d) should occur in atomic kaon experiments, where the K^- has a low energy but where a larger nucleus is used and the remaining nucleus may absorb the virtual pion.

The $K^- \bullet N \bullet N$ binding is suggested by the deuteron ${}^{2}H$, a proton-neutron bound-state, and by the model of the $\Lambda(1405)$ as an antikaon proton bound-state. However the subtleties of these two-body subsystems require a precise computation of the binding energy of the three-body system. For instance the binding of the deuteron ($p \bullet n$) requires a d-wave component [3]. Moreover it is not clear yet if the $K^- \bullet N$ binds in an $I = 1$ Σ baryon. Notice that in the $I = 0$ channel there is strong evidence that the $\Lambda(1405)$ is constituted of two poles, respectively, dominated by the $K^- \bullet N$ and the $\pi \bullet \Sigma$ channels [4–11].

The $K^- \bullet N \bullet N$ binding is a very recent topic. While Oset, Toki, and collaborators [12,13] offer a different interpretation to the FINUDA peak, very recent theoretical calculations, fitting the $K^- \bullet N$ scattering data with effective local potentials [14–16] or with separable potentials [17] agree with a relatively deep and wide $K^- \bullet N \bullet N$ resonance.

Here we specialize in the microscopic quark computation of the binding energy and width of the $K^- \bullet N \bullet N$ systems. Section II is dedicated to the $N \bullet N$ and $K \bullet N$ interactions. We compute microscopically the $K \bullet N$ interaction, with a confining and chiral invariant quark model and using the Resonating Group method (RGM). In Sec. III

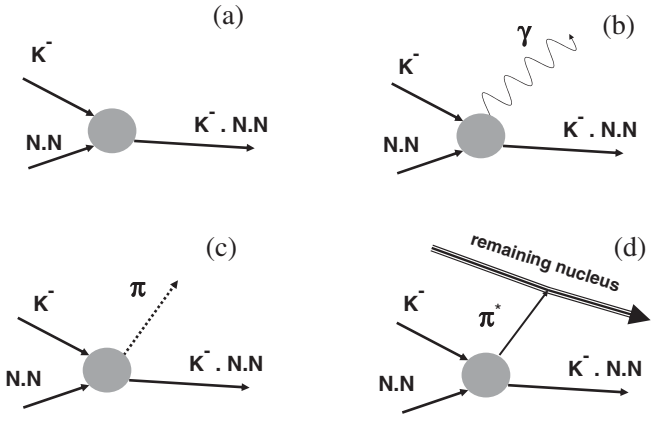

FIG. 1. Different $K^- \bullet N \bullet N$ production mechanisms.

we calibrate our interactions with the experimental $K^+ \bullet N$ data, and we study the binding and decay of $K^- \bullet N$ and $K^- \bullet N \bullet N$ systems. Finally we conclude.

II. FROM QUARKS TO THE $K \bullet N$

There are several very precise models of the $N \bullet N$ interaction [3], compatible with the experimental $N \bullet N$ phase shifts. All contain a long-range attractive potential, a medium-range attractive potential, and a hard core or short range potential. A picture consistent with QCD emerges if the long range attraction is due to the Yukawa one-pion exchange, the medium range is due to two-pion or one-sigma exchange, while the short range repulsion is dominated by the quark interactions. Different models exist because the $^3S_1 \leftrightarrow {}^3D_1$ coupling is partly equivalent to the attractive part of the $^3S_1$ potential. Moreover the repulsive hard core potential essentially pushes the wave function outside the repulsive core region, and this can be accomplished for different heights of the repulsive core. Also, separable or local potentials can be used.

However the $K^- \bullet N$ interaction has not yet been modeled with the same detail of the $N \bullet N$ interaction [18]. Notice that not only the kaons are unstable particles, with less experimental results, but also there are large inelastic coupled channel effects in the $K^- \bullet N$ scattering. Moreover, there is strong evidence that the $\Lambda(1405)$ does not have a single pole with width Γ of 40 MeV, but two narrower poles, one closer to the $K^- \bullet N$ threshold and another dominated by the $\pi \bullet \Sigma$ channel.

This leads us to compute the $K^- \bullet N$ interaction microscopically at the quark level. Here we assume a standard quark model (QM) Hamiltonian,

$$H = \sum_i T_i + \sum_{i<j,\bar{i}<\bar{j}} V_{ij} + \sum_{i,\bar{j}} A_{i\bar{j}}, \tag{1}$$

where each quark or antiquark has a kinetic energy T_i with a constituent quark mass, and the color dependent two-body interaction V_{ij} includes the standard QM confining term and a hyperfine term,

$$V_{ij} = \frac{-3}{16} \vec{\lambda}_i \cdot \vec{\lambda}_j [V_{\rm conf}(r) + V_{\rm hyp}(r) \vec{S}_i \cdot \vec{S}_j]. \tag{2}$$

For the purpose of this paper the details of potential (2) are unimportant; we only need to estimate its matrix elements. The hadron spectrum is compatible with

$$\langle V_{\rm hyp} \rangle \simeq \tfrac{4}{3}(M_\Delta - M_N). \tag{3}$$

Moreover we include in the Hamiltonian (1) a quark-antiquark annihilation potential $A_{i\bar{j}}$. Notice that the quark-antiquark annihilation is constrained when the quark model produces spontaneous chiral symmetry breaking [19–24]. In the π Salpeter equation, the annihilation potential A cancels most of the kinetic energy and confining potential $2T + V$,

$$\langle A \rangle_{S=0} \simeq \langle 2T + V \rangle_{S=0} \simeq \langle V_{\rm hyp} \rangle, \tag{4}$$

leading to a massless pion in the chiral limit. We stress that the QM of Eq. (1) not only reproduces the meson and baryon spectra as quark and antiquark bound-states, but it also complies with the PCAC theorems [22–26].

For the pentaquark system, the RGM [27] is convenient to arrange the wave functions of quarks and antiquarks in antisymmetrized overlaps of simple color singlet quark clusters, the baryons, and mesons. The effective potential of the meson-baryon system is computed with the overlap of the intercluster microscopic potentials,

$$V_{\substack{\text{bar } A \\ \text{mes } B}} = \langle \phi_B \phi_A | - (V_{14} + V_{1\bar{5}} + 2V_{24} + 2V_{2\bar{5}}) 3P_{14} + 3A_{1\bar{5}} | \phi_A \phi_B \rangle / \langle \phi_B \phi_A | 1 - 3P_{14} | \phi_A \phi_B \rangle, \tag{5}$$

where P_{ij} stands for the exchange of particle i with particle j, see Fig. 2. This results in an algebraic color $\times$ spin $\times$ flavor factor and a spatial overlap. A convenient basis for the spatial wave functions of the meson A and the baryon B is the harmonic oscillator basis,

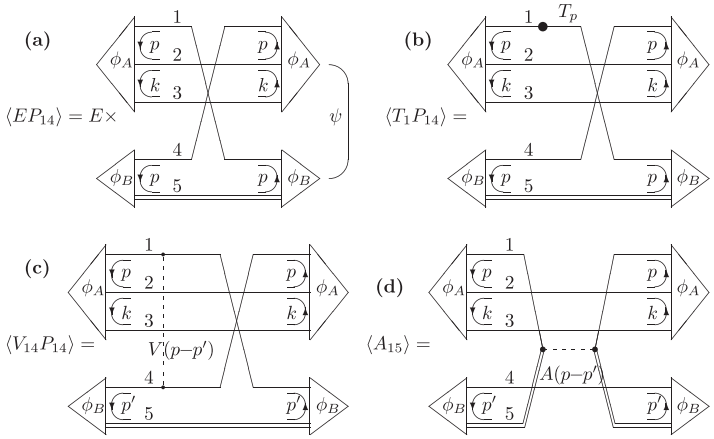

FIG. 2. Examples of our RGM overlaps for the baryon-meson effective interaction: (a) norm exchange overlap; (b) kinetic exchange overlap; (c) interaction exchange overlap; (d) annihilation overlap.

$$\phi^{\alpha}_{000}(\rho) = {\mathcal{N}_{\alpha}}^{-1} \exp\left(-\frac{\rho^2}{2\alpha^2}\right), \qquad \mathcal{N}_{\alpha} = (\sqrt{\pi}\alpha)^{3/2}. \quad (6)$$

In what concerns the quark exchange diagrams, the spin independent part of the quark-quark(antiquark) potential in Eq. (2) essentially vanishes because the clusters are color singlets. The only potential which may contribute is the hyperfine potential. The quark Pauli exchange also leads to a positive, repulsive potential.

Importantly, each annihilation diagram can be related to an exchange diagram with the crossing symmetry of one of the incoming baryon with the outgoing baryon. This is evident in Figs. 2(c) and 2(d). The corresponding diagrams are opposite because the annihilation diagram does not have the Pauli exchange minus sign of the exchange diagram. Another important difference occurs, the exchange diagrams produce nonlocal simple separable potentials, while the annihilation diagrams produce simple local Gaussian potentials. Nevertheless all the different diagrams produce hard core potentials proportional to $\langle V_{\rm hyp}\rangle$, repulsive in exchange diagrams and attractive in annihilation diagrams. Notice that attraction may only occur in nonexotic channels.

We summarize [28–32] the effective potentials computed for the relevant channels,

$$\begin{aligned}
V_{K\bullet N} &= c_K^2 \langle V_{\rm hyp}\rangle \tfrac{23}{32}(1 + \tfrac{20}{23}\vec{\tau}_K \cdot \vec{\tau}_N)|\phi^{\alpha}_{000}\rangle\langle\phi^{\alpha}_{000}|, \\
V_{\bar{K}\bullet N}(\mathbf{r}) &= -c_K^2 \langle V\rangle 2\sqrt{2}(1 - \tfrac{4}{3}\vec{\tau}_K \cdot \vec{\tau}_N)e^{-r^2/\alpha^2}, \\
V_{\bar{K}\bullet N \leftrightarrow \pi\bullet\Lambda} &= c_\pi c_K \langle V_{\rm hyp}\rangle \tfrac{9}{32}(1 + \tfrac{4}{3}\vec{\tau}_K \cdot \vec{\tau}_N)|\phi^{\alpha}_{000}\rangle\langle\phi^{\alpha}_{000}|, \\
V_{\bar{K}\bullet N \leftrightarrow \pi\bullet\Sigma} &= c_\pi c_K \langle V_{\rm hyp}\rangle \tfrac{-5}{8}(\tfrac{1+\sqrt{6}}{4} + \tfrac{-3+\sqrt{6}}{3}\vec{\tau}_K \cdot \vec{\tau}_N)|\phi^{\alpha}_{000}\rangle \\
&\quad \times \langle\phi^{\alpha}_{000}|, \qquad (7)
\end{aligned}$$

where $\vec{\tau}$ are $1/2$ of the Pauli isospin matrices for the $I = 0$ and $I = 1$ cases, $c_\pi = \sqrt{E_\pi} f_\pi (\sqrt{2\pi}\alpha)^{3/2}/\sqrt{3}$ is a PCAC factor, and $\mathbf{r}$ is the relative coordinate.

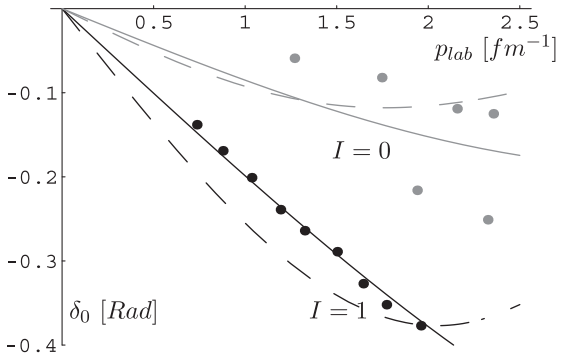

FIG. 3. $I = 0$ (gray) and $I = 1$ (black) s-wave $K \bullet N$ phase shifts as a function of the kaon momentum in the laboratory frame. The dots are experimental [33–35] and the solid lines represent this model [28–32] with the hadronic size parameter $\alpha = 0.36$ fm and ${c_k}^2 V_{\rm hyp} = 436/\sqrt{8} = 250$ MeV. A much larger $\alpha = 0.66$ fm, even with a small ${c_k}^2 V_{\rm hyp} = 45$ MeV potential strength, would produce a worse fit (dashed line).

We calibrate our parameters in the two-body $K \bullet N$ channels, where the diagonalization of the finite difference Hamiltonian is straightforward. From baryon spectroscopy we get $\langle V_{\rm hyp}\rangle = 390$ MeV. Since c_K is a PCAC factor that suppresses the norm of quasi-Golstone-bosons, consistent with the Adler zero in the chiral limit, we get the plausible parameter interval $c_k^2\langle V_{\rm hyp}\rangle \in [200, 300]$ MeV. From the phase shifts for the first channel of Eq. (7), the repulsive and well understood $S = 1$ $K \bullet N$ channel [33–35] depicted in Fig. 3, we determine the size parameter $\alpha \in [0.34, 0.39]$ fm. This is necessarily smaller, by a factor of 2, than the hadronic charge radius which is enhanced by the vector meson dominance.

III. RESULTS AND CONCLUSION

To study the binding and decay of the $K^- \bullet N$ two-body systems and of the $K^- \bullet N \bullet N$ three-body systems, we diagonalize the Hamiltonian in configuration space. Importantly, the decay widths to the channels $\pi \bullet \Sigma$ and $\pi \bullet \Sigma \bullet N$ are accounted with the substitution method, resulting in an effective two-body $K^- \bullet N$ separable potential $-|\phi_{000}\rangle\langle\phi_{000}|G_0(E)|\phi_{000}\rangle\langle\phi_{000}|$. Because the energy E of our plausible resonances is the above pionic channels, the Green function matrix elements are complex. This produces the decay width contribution $-i\Gamma/2$ to the eigenvalues of the Schrödinger two-body and three-body Hamiltonians.

First we study the Λ channel with the $I = 0$ two-body $K^- \bullet N$ system. Using the PCAC ratio $c_\pi/c_K = \sqrt{E_\pi/M_K} \simeq 0.56$, and solving the $K^- \bullet N$ Schrödinger equation in this parameter range, including the coupling to the $\pi \bullet \Sigma$ effective potential, we get a resonance in the $\Lambda(1405)$ region, with binding energy $M - m_K - m_N \in [-23.8, -1.7]$ MeV, and width $\Gamma \in [3.5, 7.0]$ MeV. This is distant from the single Breit-Wigner model for the $\Lambda(1405)$ resonance, with a width of $\Gamma \simeq 40$ MeV [36] and a binding energy of -30 MeV. We also consider an increase of the chiral coupling up to $c_\pi/c_K = 1$, to simulate the possible effect of other decay channels. Maintaining the remaining parameter ranges, the resonance approaches the $\Lambda(1405)$ region, with binding energy $M - m_K - m_N \in [-42.2, -7.7]$ MeV, and width $\Gamma \in [11.2, 23.0]$ MeV. This is reasonably close to the $\Lambda(1405)$, possibly also close to its double pole models, including a slightly narrower Breit-Wigner pole closely below the $K^- \bullet N$ threshold (here we do not address the second pole, since for simplicity we did not include the $\pi \bullet \Sigma$ interaction, less relevant for the $K^- \bullet N \bullet N$ system).

It is then instructive to find how much we can decrease the $I = 0$ attraction, and still bind the $K^- \bullet N$ system. Excluding the coupled channels, the $V_{K^-\bullet N}$ attraction is marginally sufficient to bind the $I = 0$ system, up to a 1 MeV binding energy. The coupled channel effects further bind the system and, even if the overall $I = 0$ attraction is reduced by a factor $\in [0.77, 0.89]$, binding occurs.

In the Σ channel with the $I = 1$ two-body $K^- \bullet N$ system, according to Eq. (7), the $V_{K^-\bullet N}$ attraction is decreased by a factor of $\frac{1}{3}$, when compared with the $I = 0$ channel. Clearly, this small potential is far from being able to bind the $K^- \bullet N$ onto a Σ.

We finally study the $K^- \bullet N \bullet N$ three-body system, using the Nijmegen REID93 potential [3], together with our $K^- \bullet N$ interaction and our coupling to the $\pi \bullet \Sigma$ and $\pi \bullet \Lambda$ channels. Importantly, our two-body subsystems only bind for isospin $I = 0$. For the $N \bullet N$ subsystem we can either have isospin $I_{NN} = 0$ and spin $S_{NN} = 1$, or $I_{NN} = 1$ and $S_{NN} = 0$. The two different total $I = \frac{1}{2}$ systems are, respectively, the $(-K^- pn + K^- np)/\sqrt{2}$ with spin 1, and the $(2\bar{K}_0 nn - K^- pn - K^- np)/\sqrt{6}$ with spin 0. In the $S = 1$ case, each $K^- \bullet N$ subsystem is $\frac{1}{4}$ in a Λ-like $I = 0$ state and $\frac{3}{4}$ in a Σ-like $I = 1$ state. In the $S = 0$ case, each $K^- \bullet N$ subsystem is $\frac{3}{4}$ in a Λ-like $I = 0$ state and $\frac{1}{4}$ in a Σ-like $I = 1$ state. Let us now consider the case where the two nucleons would be superposed, and use Eq. (7) to estimate the attraction that this dinucleon would impose on the antikaon. In the $S = 1$ system, the K^- would feel an attraction identical to the one it feels in the Λ system. In the $S = 0$ system, the K^- would feel a larger attraction.

Nevertheless a quantitative study is necessary because the nucleons are strongly repelled at short distance, and their separation weakens the attraction of the antikaon. It is then convenient to replace the coordinates of the three hadrons N_1, N_2, and $K^-{}_3$ by relative and center of mass coordinates

$$\begin{pmatrix} \mathbf{r}_{12} \\ \mathbf{r}_{123} \\ \mathbf{R} \end{pmatrix} = \begin{pmatrix} 1 & -1 & 0 \\ \frac{1}{2} & \frac{1}{2} & -1 \\ \frac{1}{2+\gamma} & \frac{1}{2+\gamma} & \frac{\gamma}{2+\gamma} \end{pmatrix} \begin{pmatrix} \mathbf{r}_{\mathbf{N}1} \\ \mathbf{r}_{\mathbf{N}2} \\ \mathbf{r}_{\mathbf{K}3} \end{pmatrix}, \tag{8}$$

where $\gamma = m_K/m_N$. The coordinate $\mathbf{R}$ is eliminated in the center of mass frame, and we rewrite the Hamiltonian in terms of scalar products of $\mathbf{r}_{12}$, $\mathbf{r}_{123}$ and their momenta $\mathbf{p}_{12}$ and $\mathbf{p}_{123}$. The total kinetic energy

$$T = \frac{1}{2}\frac{2}{m_N}\mathbf{p}_{12}{}^2 + \frac{1}{2}\frac{2+\gamma}{2\gamma m_N}\mathbf{p}_{123}{}^2, \tag{9}$$

is diagonal in $\mathbf{p}_{12}$ and $\mathbf{p}_{123}$. The $V_{N_1N_2}$ potential only depends on $\mathbf{r}_{12}$, including the tensor interaction. The sum of the other potentials $V_{N_1K_3} + V_{N_2K_3}$ is a function of r_{12}, r_{123} and of the square of $\omega = \hat{r}_{12} \cdot \hat{r}_{123}$. To span the possible quantum numbers of the $K^- \bullet N \bullet N$ system, we apply the total potential energy to a ground-state product of s-wave wave functions of $\mathbf{r}_{12}$ and of $\mathbf{r}_{123}$. In what concerns the angular quantum numbers, the tensor part of the $N \bullet N$ interaction $V_{N_1N_2}$ will couple the s-wave in $\mathbf{r}_{12}$ to a d-wave. The other two potentials $V_{N_1K_3} + V_{N_2K_3}$ couple the ground-state s-wave product to wave functions with any even power of ω. We address the binding of the three-body $K^- \bullet N \bullet N$ system with two different applications of the variational method. In the first method, we use a basis of Laguerre polynomials in the radial variables r_{12} and r_{123},

$$\nu_{nl}^{\alpha}(r) = \sqrt{\frac{2^{3+2l}n!}{(n+2+2l)!}}\frac{r^{1+l}}{\alpha^{3/2+l}}e^{-r/\alpha}L_n^{2+2l}\left(2\frac{r}{\alpha}\right), \tag{10}$$

adequate to study weakly bound systems, together with a basis of Legendre polynomials $P_l(\omega)$ in the angular variable w. We use up to 10 excitations in each Laguerre basis and 5 excitations in the Legendre basis, sufficient to get for instance the deuteron binding. In the second method we use a finite difference method, with 40 excitations in each of the radial variables, and 3 in the angular variable.

We now study the $I = 1/2$, $S = 1$ channel, where the ground-state has binding in the r_{12} coordinate, but no binding in the r_{123} coordinate. In particular, the r_{12} part of the wave function is localized and reproduces the deuteron wave function, while the r_{123} part is extended over the whole size of the large box where we quantize the wave function. In the limit where the size of the box is infinite, we get a bound deuteron $p \bullet n$ and a free K^-.

To study in more detail how far we are from binding, we consider the adiabatic limit of the $I = 1/2$, $S = 1$ system, where the positions of the two nucleons are frozen, by fixing the r_{12} variable. Then the energy of the kaon K^- can be computed, diagonalizing in detail the terms in the Hamiltonian depending on r_{123} and w. The resulting smaller eigenvalue of $T_{123} + T_w + V_{N_1K_3} + V_{N_2K_3}$ is shown in Fig. 4, using the parameters in our interval that provide the strongest possible binding. It occurs that the antikaon is bound to this frozen deuteron system only if $r_{12} < 2.0$ fm.

Notice that this is much smaller than the deuteron double radius mean square $\sqrt{\langle r_{12}^2 \rangle} = 3.9$ fm, which is quite large because at short distances the $N \bullet N$ subsystem suffers a strong repulsion and because the deuteron is weakly bound. Thus is would be very hard to contract the deuteron to a sufficiently small radius to bind the antikaon. Then, at

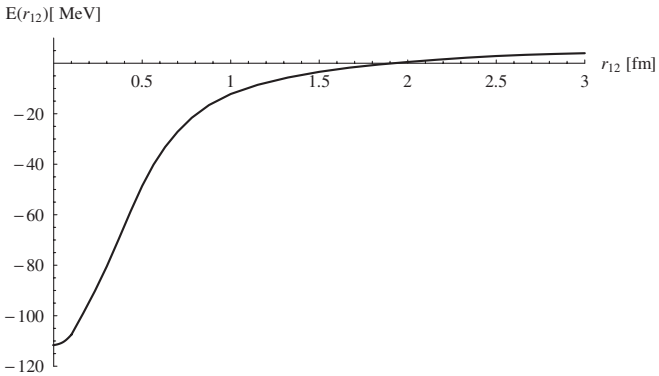

FIG. 4. Kaon energy, or real part of the lowest s-wave eigenvalue of $T_{123} + T_w + V_{N_1K_3} + V_{N_2K_3}$, as a function of the nucleon-nucleon distance $r_{12} = |r_{N_1} - r_{N_2}|$. This result is obtained in a large sphere with a r_{123} radius of 7.5 fm. In the infinite sphere radius limit the energy essentially vanishes for $r_{12} > 2.0$ fm.

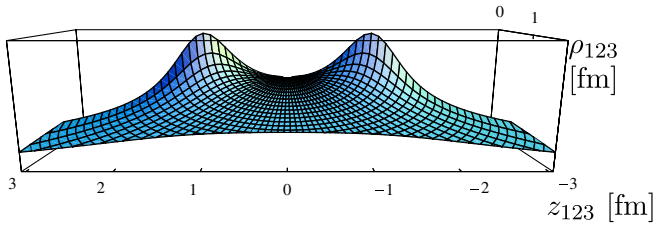

FIG. 5 (color online). 3d perspective of the antikaon wave function, assuming two adiabatically frozen nucleons at the distance of $r_{12} = 2.5$ fm, obtained with polar coordinates for the $\mathbf{r}_{123}$, with finite differences, and with a radial lattice spacing of 0.1 fm. In this unbound case, the wave function is a deformation of the lowest positive energy harmonic.

these large distances, the antikaon essentially feels a double-well potential, as shown in Fig. 5. Importantly, such a widely separated double-well potential only binds if any of the two wells is sufficiently deep to bind the antikaon. It occurs that this already happens if the $K^- \bullet N$ attraction in the $S = 1$ three-body system is arbitrarily increased by a factor $\in [1.14, 1.35]$. This produces a decay width of $\Gamma \in [8.0, 9.8]$ MeV.

This can also be applied to the $S = 0$, $K^- \bullet N \bullet N$ three-body system, where the attraction in the $K^- \bullet N$ subsystems is increased by a factor $\frac{5}{3}$ when compared with the $S = 1$ system. In particular we find a binding energy $M - m_K - 2m_N \in [-53.0, -14.2]$ MeV, and a decay width $\Gamma \in [13.6, 28.3]$ MeV to the $\pi \bullet \Sigma \bullet N$ and $\pi \bullet \Lambda \bullet N$ channels.

To conclude we compute, starting at the quark level, the $K^- \bullet N$ interactions, constrained by chiral symmetry and by the crossing symmetry to the $K^+ \bullet N$ system. We find binding in the $I = 0$, $K^- \bullet N$ channel, possibly consistent with the double pole model of the $\Lambda(1405)$, and no binding in the $I = 1$, $K^- \bullet N$ two-body Σ. In the $I = 1/2$, $S = 1$, $K^- \bullet N \bullet N$, and $S = 0$, $K^- \bullet N \bullet N$ three-body systems, we respectively find no binding, and binding.

ACKNOWLEDGMENTS

P. B. thanks Avraham Gal for an algebraic correction, Eulogio Oset and Paola Gianotti for discussions on the $K^- \bullet N \bullet N$ systems, and Marco Cardoso and George Rupp for support on the $N \bullet N$ interaction.

[1] M. Agnello *et al.* (FINUDA Collaboration), Phys. Rev. Lett. **94**, 212303 (2005).
[2] M. Agnello *et al.*, arXiv:nucl-ex/0606021.
[3] V. G. J. Stoks, R. A. M. Klomp, C. P. F. Terheggen, and J. J. de Swart, Phys. Rev. C **49**, 2950 (1994); online codes at http://nn-online.org.
[4] V. K. Magas, E. Oset, and A. Ramos, Phys. Rev. Lett. **95**, 052301 (2005).
[5] J. A. Oller and U. G. Meissner, Phys. Lett. B **500**, 263 (2001).
[6] D. Jido, A. Hosaka, J. C. Nacher, E. Oset, and A. Ramos, Phys. Rev. C **66**, 025203 (2002).
[7] C. Garcia-Recio, J. Nieves, E. Ruiz-Arriola, and M. J. Vicente-Vacas, Phys. Rev. D **67**, 076009 (2003).
[8] D. Jido, J. A. Oller, E. Oset, A. Ramos, and U. G. Meissner, Nucl. Phys. **A725**, 181 (2003).
[9] C. Garcia-Recio, M. F. M. Lutz, and J. Nieves, Phys. Lett. B **582**, 49 (2004).
[10] T. Hyodo, S. I. Nam, D. Jido, and A. Hosaka, Phys. Rev. C **68**, 018201 (2003).
[11] S. I. Nam, H. C. Kim, T. Hyodo, D. Jido, and A. Hosaka, J. Korean Phys. Soc. **45**, 1466 (2004).
[12] E. Oset and H. Toki, Phys. Rev. C **74**, 015207 (2006).
[13] V. K. Magas, E. Oset, A. Ramos, and H. Toki, Phys. Rev. C **74**, 025206 (2006).
[14] A. N. Ivanov, P. Kienle, J. Marton, and E. Widmann, arXiv:nucl-th/0512037.
[15] T. Yamazaki and Y. Akaishi, arXiv:nucl-ex/0609041.
[16] T. Yamazaki and Y. Akaishi, arXiv:nucl-th/0604049.
[17] N. V. Shevchenko, A. Gal, and J. Mares, Phys. Rev. Lett. **98**, 082301 (2007).
[18] Y. Akaishi and T. Yamazaki, Phys. Rev. C **65**, 044005 (2002).
[19] P. Bicudo and J. E. Ribeiro, Phys. Rev. D **42**, 1611 (1990); **42**, 1625 (1990); **42**, 1635 (1990).
[20] P. Bicudo, Phys. Rev. C **60**, 035209 (1999).
[21] F. J. Llanes-Estrada and S. R. Cotanch, Phys. Rev. Lett. **84**, 1102 (2000).
[22] P. Bicudo, Phys. Rev. C **67**, 035201 (2003).
[23] P. Bicudo, S. Cotanch, F. Llanes-Estrada, P. Maris, J. E. Ribeiro, and A. Szczepaniak, Phys. Rev. D **65**, 076008 (2002).
[24] P. Bicudo, M. Faria, G. M. Marques, and J. E. Ribeiro, Nucl. Phys. **A735**, 138 (2004).
[25] R. Delbourgo and M. D. Scadron, J. Phys. G **5**, 1621 (1979).
[26] F. J. Llanes-Estrada and P. Bicudo, Phys. Rev. D **68**, 094014 (2003).
[27] J. Wheeler, Phys. Rev. **52**, 1083 (1937); **52**, 1107 (1937).
[28] P. Bicudo and J. E. Ribeiro, Z. Phys. C **38**, 453 (1988).
[29] P. Bicudo, J. E. Ribeiro, and J. Rodrigues, Phys. Rev. C **52**, 2144 (1995).
[30] P. Bicudo, Nucl. Phys. **A748**, 537 (2005).
[31] P. Bicudo, Phys. Rev. D **70**, 111504(R) (2004).
[32] P. Bicudo, Phys. Rev. D **74**, 036008 (2006).
[33] J. S. Hyslop, R. A. Arndt, L. D. Roper, and R. L. Workman, Phys. Rev. D **46**, 961 (1992).
[34] T. Barnes and E. Swanson, Phys. Rev. C **49**, 1166 (1994).
[35] R. A. Arndt, I. I. Strakovsky, and R. L. Workman, Int. J. Mod. Phys. A **18**, 449 (2003); online codes at http://gwdac.phys.gwu.edu.
[36] K. Hagiwara *et al.* (Particle Data Group Collaboration), Phys. Rev. D **66**, 010001 (2002).